Laboratory Investigation (2011) 91, 704–710

Carnitine is necessary to maintain the phenotype and function of brown adipose tissue

Kiyokazu Ozaki, Tomoya Sano, Naho Tsuji, Tetsuro Matsuura and Isao Narama

The juvenile visceral steatosis (JVS) mouse is a mutant strain with an inherited systemic carnitine deficiency. Mice of this strain show clinical signs attributable to impaired heat production and disturbed energy production. Brown adipose tissue (BAT) is the primary site of non-shivering thermogenesis in the presence of uncoupling protein-1 (UCP-1) in rodents and humans, especially in infants. To investigate the possible cause of impaired heat production in BAT, we studied the morphological features, carnitine concentration, and UCP-1 production of BAT in JVS mice. The effect of carnitine administration on these parameters was also examined. JVS mice aged 5 or 10 days (60 each) and age-matched control mice were used in this study, along with 10-day-old JVS mice treated subcutaneously with L-carnitine once a day between postpartum days 5 and 10. JVS mice showed lower body temperatures and lower concentrations of carnitine in BAT. Morphologically, BAT cells in JVS mice contained large lipid vacuoles and small mitochondria, similar to those present in white adipose tissue cells. In addition, UCP-1 mRNA and protein expression levels were significantly reduced in JVS as compared with control mice. Carnitine treatment resulted in significant increases in body temperature and carnitine concentrations in BAT, together with the recovery of normal morphological features. UCP-1 mRNA and protein expression levels were also significantly increased. These findings strongly suggest that carnitine is essential for maintaining the function and morphology of BAT.

Laboratory Investigation (2011) **91,** 704–710; doi:10.1038/labinvest.2011.6; published online 14 February 2011

KEYWORDS: brown adipose tissue; carnitine deficiency; fatty acid oxidation; mitochondria; uncoupling protein-1

Brown adipose tissue (BAT) is the primary site of non-shivering thermogenesis. Heat production is carried out in the presence of uncoupling protein-1 (UCP-1).[1] UCP-1 localizes to the mitochondrial inner membrane and uncouples proton entry from ATP synthesis.[1,2] Previous studies have reported that decreased expression of UCP-1 caused by various conditions such as fasting, deletion of the UCP-1 gene, and obesity (eg, *ob/ob* and *db/db* mice) induces a low body temperature resulting from the impaired thermogenesis in BAT.[3–8]

Carnitine has been widely distributed in various tissues and organs throughout the body, including BAT, and it has an essential role in the transfer of long-chain fatty acids into the mitochondria for β-oxidation.[9] When a carnitine deficiency develops, long-chain fatty acids are not available for β-oxidation and energy production, thereby causing excessive lipid accumulation in skeletal muscle, heart, and liver and ultimately, leading to cardiac myopathy and hepatomegaly.[9,10] The juvenile visceral steatosis (JVS) mouse is a mutant animal model of systemic carnitine deficiency caused by mutation of the *OCTN2* gene, which encodes a plasma membrane carnitine transporter.[11] The JVS phenotype is inherited in an autosomal recessive manner and is characterized by growth retardation, fatty liver, hypoglycemia, hyperammonemia, and cardiac hypertrophy.[12–19] Carnitine administration improves the characteristic symptoms of JVS mice.[15,17,18,20] Moribund JVS mice display continuous shivering, which is attributable to a decrease in heat production and an enhanced sensitivity to cold.[12]

In a previous study, we demonstrated that the morphology of BAT in JVS mice resembles that of white adipose tissue (WAT), in which the adipocytes contain large fat droplets. This finding suggests that the tissue is in a hypoactive state.[12]

In the present study, we examined the morphological features of BAT and UCP-1 production in the BAT cells of JVS mice to elucidate the changes caused by carnitine deficiency and the effects of carnitine administration.

Department of Pathology, Faculty of Pharmaceutical Science, Setsunan University, Hirakata, Osaka, Japan
Correspondence: Dr K Ozaki, Department of Pathology, Faculty of Pharmaceutical Science, Setsunan University, 45-1 Nagaotohge-cho, Hirakata, Osaka 5730101, Japan.
E-mail: ozaki@pharm.setsunan.ac.jp

Received 26 July 2010; revised 15 November 2010; accepted 2 December 2010

MATERIALS AND METHODS

Animals

JVS mice (*jvs/jvs*) were originally identified as mutant mice in the C3H. OH strain background with a yellowish discoloration of the liver.[16] The *jvs* locus was mapped to mouse chromosome 11 by linkage analysis.[21] The *jvs* gene was introduced into C57BL/6 mice using a backcross breeding system to obtain JVS mice with good viability and fertility. The JVS mutant line was maintained by mating heterozygous mutants (*jvs*/+) under specific pathogen-free conditions. A JVS mouse can be distinguished from heterozygous (+/*jvs*) or wild type (+/+) littermates by its swollen, yellowish liver, which can be visualized through the abdominal wall 5 days after birth. Heterozygous mutants were further discriminated from wild type (+/+) animals using microsatellite marker analysis.[21] The mice used in the present study were housed in an air-conditioned animal room, and suckled by mother mice during experimental period. Mother mice were fed a standard laboratory diet, and supplied water *ad libitum*. Sixty male JVS and sixty male control mice were used. Animal subjects consisted of 5- or 10-day-old JVS mice, 10-day-old JVS mice treated with carnitine and age-matched isogenic wild type mice as controls. Animals in the carnitine treatment group were subcutaneously injected with 1 mg of L-carnitine–HCl (Sigma, St Louis, MO, USA) once a day from postpartum days 5–10. On postpartum day 10, rectal body temperatures were measured using a thermistor (Takara Thermistor Instruments, Yokohama, Japan). All the procedures used for animal handling and experimental treatments were in accordance with the Guidelines for the Care and Use of Laboratory Animals from the Committee for Animal Experiments of Setsunan University and the Japanese Association for Laboratory Animal Science.

Total Carnitine Assay

Fifteen male JVS and 15 male control mice were deeply anesthetized and perfused with physiological saline at the age of 5 or 10 days. Tissue samples containing BAT were excised, and 10 mg of BAT was immersed in 100 μl of homogenization buffer solution (0.25 mM sucrose, 3 mM Tris–HCl, 0.1 mM EDTA, pH 7.4) and then homogenized. The homogenate was centrifuged at 25 000 *g* for 30 min, the pellet was discarded, and the supernatant was placed in a fresh tube and filtered through a 0.45-μm filter (Milex HV, Millipore, Billerica, MA, USA). The filtrate was centrifuged in a Millipore Microcon centrifugal filter (YM-10, 10 000 MW, Millipore) for 10 min at 12 000 *g*. The filtrate was assayed for total carnitine (including acylcarnitine and free carnitine) using the enzymatic cycling method (Total carnitine 'Kainos', Kainos Laboratories, Tokyo, Japan).[22]

Light and Electron Microscopy

BAT samples for examination by light microscopy were fixed in 10% phosphate-buffered formalin (pH 7.4), processed into wax blocks, sectioned (4 μm thick) and stained with hematoxylin and eosin. Tissue fragments of BAT for electron microscopy were fixed with 2.5% glutaraldehyde in 0.1 M phosphate buffer, pH 7.4. After fixation, the tissue samples were post-fixed in 1% osmium tetroxide solution (pH 7.4) and processed into epoxy resin. Ultra-thin sections were cut and stained with uranyl acetate and lead citrate and examined under an electron microscope (JEM 1200EX, JEOL, Tokyo, Japan).

Immunohistochemical Analysis

Anti-UCP-1 rabbit polyclonal antibody (1:500, Abcam, Cambridge, UK) served as a primary antibody for immunohistochemical analysis. All the slides were rinsed with 0.05 M Tris-buffered saline (TBS, pH 7.6) containing 0.01% Tween 20, treated with 1% hydrogen peroxide and rinsed again with TBS plus Tween 20. The slides were incubated in bovine serum for 5 min and then with primary antibody overnight at 4 °C. The slides were subsequently rinsed with TBS plus Tween 20, treated for 30 min at room temperature with N-Histofine mouse MAX PO (Nichirei, Tokyo, Japan), rinsed with TBS plus Tween 20, incubated in diaminobenzidine solution containing 0.01% hydrogen peroxide for the peroxidase coloring reaction, and counterstained with Mayer's hematoxylin.

Western Blot Analysis

Each tissue sample (five individual samples per group) was homogenized in 10 volumes of lysis buffer (10 mM Tris–HCl, pH 7.4, 1 mM EDTA, 2 mM Na_3VO_4, 1 mM phenylmethylsulfonyl fluoride, and 10 μg/ml aprotinin) for 30 s using a polytron apparatus. After centrifugation at 1500 *g* for 5 min, the fat cake was discarded, and the infranant fraction (fat-free extract) was used for western blot analysis of UCP-1 levels. Briefly, the fat-free extract (10 μg protein) was solubilized, subjected to sodium dodecyl sulfate–polyacrylamide gel electrophoresis and transferred to a nitrocellulose filter. After the filter was blocked with 1% bovine serum albumin, it was incubated with anti-UCP-1 rabbit polyclonal antibody (1:8000). The filter was subsequently rinsed with TBS plus Tween 20, treated for 60 min at room temperature with N-Histofine mouse MAX PO (1:50, Nichirei) and rinsed with TBS plus Tween 20. The immunocomplex was detected by enhanced chemiluminescence detection (ECL, GE HealthcareUK, Buckinghamshire, UK).

Real-Time RT–PCR

Total RNA was extracted from BAT using the RNeasy Mini Kit (QIAGEN, Hilden, Germany) and stored at −80 °C. Adipose RNA was reverse-transcribed using the First-Strand cDNA Synthesis Kit (GE Healthcare UK) to generate cDNA. The cDNA was then subjected to quantitative real-time PCR (10 ng per reaction) carried out with TaqMan Universal PCR Master Mix (Life Technologies, Carlsbad, CA, USA) using the 7300 Real-Time PCR System (Life Technologies) with predeveloped TaqMan probe/primer combinations for UCP-1

(Mm00494069_m1) and glyceraldehyde-3-phosphate dehydrogenase (Mm99999915_g1) optimized by the manufacturer. Threshold cycle numbers were transformed using the *Ct* and relative value method as described by the manufacturer and were expressed relative to glyceraldehyde-3-phosphate dehydrogenase, which was used as a housekeeping gene.

Data Analysis

Data are presented as mean values ± 1s.d. One-way ANOVA with Tukey's multiple comparisons test was used to determine significant differences. When the calculated *P*-value was <0.05, the difference was considered statistically significant. Statistical analyses were performed using the StatMate III program (ATMS, Tokyo, Japan).

RESULTS

Clinical Signs, Body Weight, and Body Temperature

Clinically, 5-day-old JVS mice were almost indistinguishable from control mice. Ten-day-old JVS mice displayed growth retardation and significantly lower body weights as compared with controls (Table 1). In contrast, 10-day-old JVS mice treated with carnitine appeared normal by clinical observation and gained body weight comparably to control mice.

Table 1 Body weight and body temperature of control and JVS mice

	Body weight (g)		Body temperature (°C)	
	Mean	s.d.	Mean	s.d.
5-day-old				
Control	3.36	0.39	ND	
JVS	2.92	0.45	ND	
10-day-old				
Control	5.23	0.40	34.88	0.57
JVS	4.33	0.44[a,b]	32.00	1.54[c,b]
JVS+carnitine	5.53	0.54	35.15	0.61

[a] $P<0.01$ *vs* 10-day-old control mice.
[b] $P<0.01$ *vs* 10-day-old JVS mice with carnitine treatment.
[c] $P<0.05$ *vs* 10-day-old control mice.

The rectal body temperatures of 10-day-old JVS mice were significantly lower than those of control animals (Table 1). However, carnitine treatment resulted in a significant rise in body temperature to the level observed in control mice. The total carnitine concentration was significantly reduced in the BAT of 10-day-old JVS mice as compared with controls (Figure 1). Carnitine treatment induced a significant elevation of the BAT carnitine concentration to levels detected in control mice.

Light and Electron Microscopy

BAT from 5- and 10-day-old control mice showed typical features characterized by normal brown adipose cells containing many small multilocular lipid droplets and centrally located, round nuclei with weakly eosinophilic cytoplasm (Figures 2a and c). The BAT of 5-day-old JVS mice was composed of adipose cells containing larger lipid droplets than those of control mice, but these samples also contained many small droplets (Figure 2b). In the BAT of 10-day-old JVS mice, almost all cells included large, unilocular lipid droplets and only a few small lipid droplets (Figure 2d). The nuclei were elongated and located eccentrically. These cell features were similar to those of WAT. Carnitine treatment caused a decrease in the number of large lipid droplets in brown adipocytes (Figure 2e). The morphological features of each brown adipocyte were similar to those of adipocytes from control animals (Figure 2e). Ultrastructurally, brown adipocytes from 5-day-old JVS mice and control mice contained numerous mitochondria with densely packed cristae

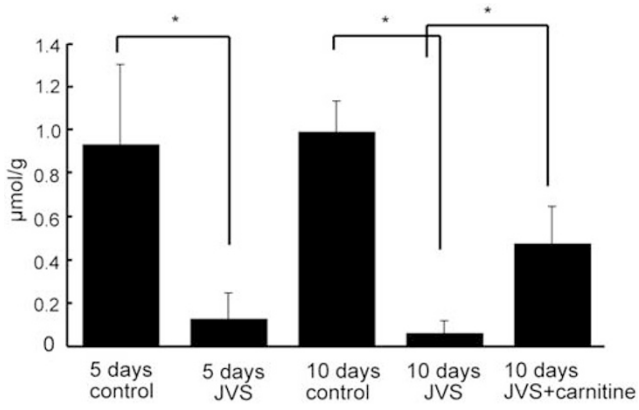

Figure 1 Total carnitine concentration in BAT. Significant differences between groups are indicated. *$P<0.01$.

Figure 2 Light and electron micrographs of BAT in control and JVS mice. BAT from 5- and 10-day-old control mice shows features typical of BAT containing small multilocular lipid droplets (**a**, **c**). Brown adipose cells from 5-day-old JVS mice contain large multilocular lipid droplets in addition to small multilocular droplets (**b**). An increased number of enlarged unilocular lipid droplets and a decreased number of small lipid droplets are observed in the BAT from 10-day-old JVS mice (**d**). Carnitine treatment decreases the number of large lipid droplets (**e**). Electron microscopy shows that 5-day-old JVS and control mice have numerous large, polyhedral mitochondria with densely packed cristae (**f** and **g**). The mitochondria of 10-day-old JVS mice are small and round with loosely packed cristae (**i**). Carnitine treatment results in a normal mitochondrial shape (**j**). Immunohistochemically, positive UCP-1 staining of samples from 5- and 10-day-old JVS mice is reduced in comparison to controls (**k**, **l** and **n**). Carnitine treatment results in an increase in positive staining to levels similar to those of controls (**m** and **o**). (**a**–**e**) HE, (**f**–**j**) uranyl acetate and lead citrate, and (**k**–**o**) UCP-1 immunohistochemistry. Bars: **a**–**e**: 20 μm, **f**–**j**: 500 nm, and **k**–**o**: 100 μm.

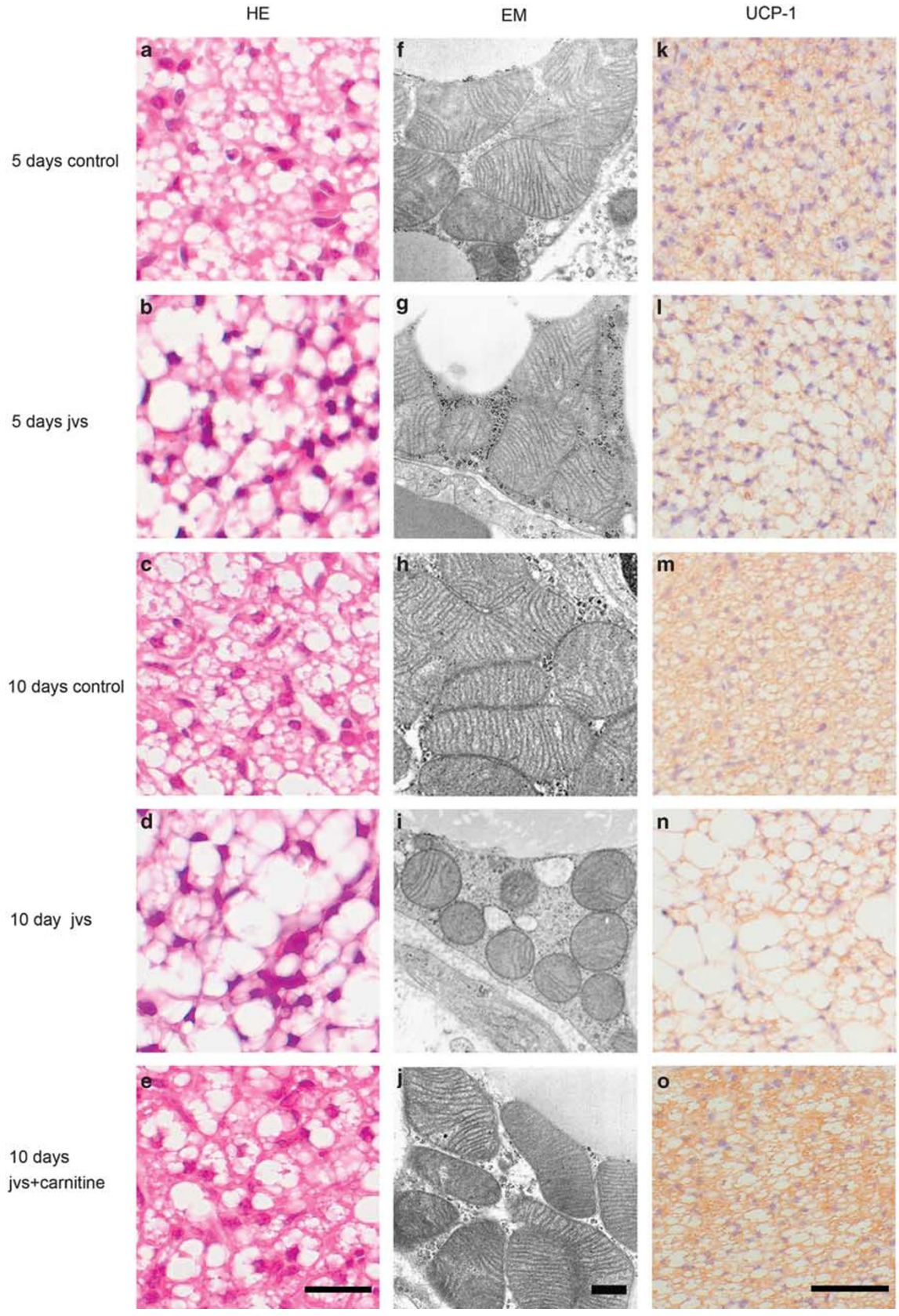
HE
EM
UCP-1
5 days control
5 days jvs
10 days control
10 day jvs
10 days
jvs+carnitine
a
b
c
d
e
f
g
h
i
j
k
l
m
n
o

Figure 3 Electron micrograph of a brown adipose cell from a 10-day-old JVS mouse without carnitine treatment. The mitochondria are extremely large and display electron-dense filaments (arrows) and myelin-like structures (arrowheads) in the matrix. The sample was stained with uranyl acetate and lead citrate. Bar: 500 nm.

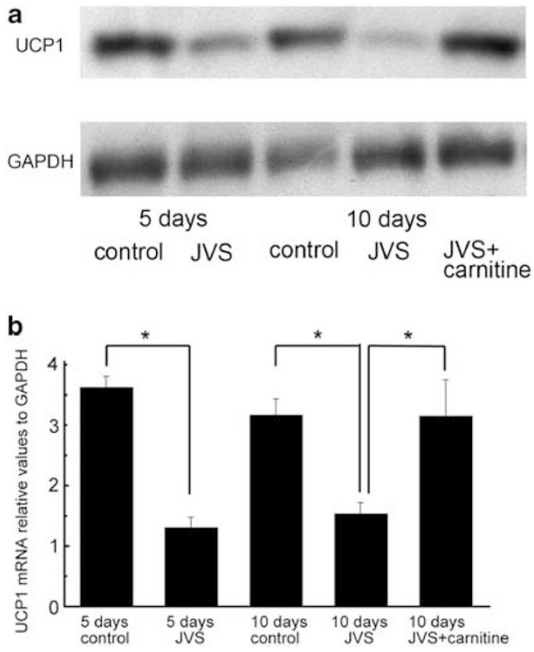

Figure 4 (**a**) Western blotting analysis of UCP-1 protein expression in the five groups. Compared with controls, 5- and 10-day-old JVS mice show markedly decreased expression of UCP-1. Carnitine treatment increases UCP-1 protein expression. (**b**) Real-time RT–PCR determination of UCP-1 mRNA levels in the five groups. Compared with those of 5- and 10-day-old control mice, UCP-1 mRNA levels in 5- and 10-day-old JVS mice are significantly decreased. Carnitine treatment significantly increases UCP-1 mRNA expression to levels similar to those found in 5- and 10-day-old control mice. Significant differences between groups are indicated. $^{*}P<0.01$.

(Figures 2f and g). These features corresponded to the eosinophilic cytoplasm detected by light microscopy and are characteristic of BAT. In contrast, most of the mitochondria of 10-day-old JVS mice were reduced in size, with a rounded morphology and loosely packed cristae (Figure 2i). These mitochondria were severely miniaturized, especially in cells containing large lipid droplets similar to those found in white adipocytes. However, giant mitochondria were infrequently observed and contained electron-dense filaments and myelin-like structures in the matrix (Figure 3). These giant mitochondria could not be detected in control mice. In the carnitine-treated animals, the mitochondria displayed a shape similar to those of control mice (Figure 2j).

Immunohistochemistry, Western Blotting, and Real-Time PCR for UCP-1

Immunohistochemically, UCP-1 positivity in samples from 5- and 10-day-old JVS mice was reduced in comparison to controls (Figures 2k, l and n). Carnitine treatment resulted in an increase in positivity to levels similar to those of the control (Figures 2m and o). UCP-1 protein expression levels in 5- and 10-day-old JVS mice showed marked decreases compared with those in 5- and 10-day-old controls by western blotting (Figure 4a). Carnitine induced a remarkable increase in UCP-1 protein expression (Figure 4a). UCP-1 mRNA levels in 5- and 10-day-old JVS mice were significantly decreased compared with those in 5- and 10-day-old controls (Figure 4b). Carnitine treatment caused a significant increase in UCP-1 mRNA expression to levels equivalent to those detected in 5- and 10-day-old control mice (Figure 4b).

DISCUSSION

The results of the present study show that carnitine is an essential compound for maintaining the cell structure typical of BAT and for generating heat in the presence of UCP-1. The excessive accumulation of lipid droplets in the BAT of carnitine-deficient JVS mice may be caused by a decreased utilization of long-chain fatty acids. Therefore, lipid droplets dramatically decrease in size, and histopathological and ultramicroscopic features are completely recovered by L-carnitine treatment. This hypothesis is also supported by the results showing that UCP-1 mRNA and protein expression, carnitine concentrations, and body temperature were also restored along with normal cell structure. Therefore, it is clear that carnitine also restores thermogenic activity in BAT.

The carnitine concentration in the BAT of JVS mice was also dramatically elevated by L-carnitine administration. Plasmalemmal carnitine uptake is known to depend on carnitine transporters. Organic cation transporter 2 (OCTN2) has been shown to transport carnitine with high-affinity and is strongly expressed in the kidney, skeletal muscle, heart, and placenta, but not in the liver.[23,24] Mutation of the *OCTN2* gene in humans causes primary systemic carnitine deficiency.[11] JVS mice also carry an *OCTN2* gene mutation[11,25]

and display a severe carnitine deficiency and the accumulation of lipid droplets in various cells (hepatocytes, renal tubular epithelial cells, cardiac myocytes, and striated myocytes).[12–14,17] L-carnitine administration increases the carnitine concentration and eliminates the accumulation of lipids in the liver, heart, and skeletal muscle of JVS mice.[12,14,17,26] However, tissue carnitine levels in the heart, liver, and skeletal muscle are significantly lower than those in controls, even after L-carnitine administration.[26] According to these previous reports, the effects of L-carnitine administration seem to differ among various organs. Differences in the effects on target organs are attributable to the primary levels of OCTN2 expression, because L-carnitine treatment causes only a slight elevation of the carnitine concentration in the heart, where OCTN2 is highly expressed, whereas a prominent increase in the concentration of carnitine is detected in the liver, where OCTN2 is poorly expressed.[26] Further evidence is provided by the finding that the reduction of lipid accumulation in the liver is more prominent than that in the heart and skeletal muscle.[12] The significant increase in the carnitine concentration and the dramatic improvement of the morphology of BAT after L-carnitine treatment suggest that BAT is capable of taking up carnitine without relying on OCTN2 as well as similar results are observed for the liver. In the liver, there were two additional low-affinity carnitine transporters, OCTN1 and $ATB^{0,+}$. Carnitine can be transported by these transporters without OCTN2 in the liver.[27–29] Therefore, BAT may be able to take up carnitine using other transporter except OCTN2.

Enlarged lipid vacuoles in BAT have been detected in animals that are fasted, have undergone denervation of the sympathetic nerves, are obese (*db/db*), or carry a knockout mutation in UCP-1, dopamine β-hydroxylase, or hormone-sensitive lipase (HSL).[4,8,30–34] The morphological transition from BAT to WAT-like tissue has been thought to reflect impaired thermogenesis in the BAT, because fasting, denervated, obese (*db/db*), UCP-1 knockout, and dopamine β-hydroxylase knockout animals display low body temperatures and/or increased cold sensitivity.[4,8,31,33,34] In contrast to these animals, HSL knockout mice are sensitive to cold and maintain a normal body temperature despite possessing similar changes in their BAT.[30,32] Therefore, an enlargement of lipid vacuoles in BAT has been shown to be independent of cold sensitivity. However, the results of the present study strongly suggest that enlarged lipid droplets in BAT reflect an impaired function or a loss of function of BAT, because the low body temperatures and BAT phenotypes were completely recovered following L-carnitine administration.

The shape of the mitochondria in the BAT of JVS mice was also similar to that of mitochondria in WAT, and the structural changes were suggestive of an accompanying low body temperature and decreased expression of UCP-1. In addition, electron-dense filaments and myelin-like structures in the mitochondrial matrix that indicate cell injury were occasionally detected in JVS mice.[35] L-carnitine administration maintained the shape of mitochondria, reflecting the function of the organelles. These data indicate that carnitine affects the phenotype of mitochondria in BAT. As a result of fasting, denervation of the sympathetic nerves or UCP-1 knockout, cristae within the mitochondria became less densely packed. However, these changes were very mild, and the typical shape of the mitochondria in BAT was maintained in these mice.[7,8,31] In contrast, the mitochondria in obese (*db/db*) mice display changes similar to those observed in carnitine-deficient JVS mice in the present study.[8,33,34] The changes observed in obese mice are hypothesized to be mediated by sympathetic nerve hypoactivity.[33,34] On the other hand, catecholamine metabolism is accelerated in JVS mice, and carnitine administration improved the phenotype and thermogenesis of JVS mice.[36] These results suggest that the mitochondrial changes were influenced greatly by carnitine deficiency but were relatively less affected by sympathetic nerve activity.

Cold sensitivity has also been reported in mouse model of fatty acid oxidation deficiency.[37–39] These mice showed normal body temperature at 24 °C, but at 4 °C, showed profound cold intolerance. Thus, impaired fatty acid oxidation resulted in cold intolerance. However, BAT of these mice had full UCP-1 activity and normal morphology. JVS mouse showed cold intolerance at 24 °C, impaired UCP-1 activity and abnormal morphology. Therefore, our data indicate that JVS mouse did not have only impaired fatty acid oxidation, but also impaired activation of UCP-1.

In conclusion, the present study indicates that carnitine is an essential compound for maintaining the phenotype and function of BAT and that BAT is capable of taking up carnitine independently of the OCTN2 carnitine transporter.

DISCLOSURE/CONFLICT OF INTEREST

The authors declare no conflict of interest.

1. Cannon B, Nedergaard J. Brown adipose tissue: function and physiological significance. Physiol Rev 2004;84:277–359.
2. Nedergaard J, Golozoubova V, Matthias A, *et al.* UCP1: the only protein able to mediate adaptive non-shivering thermogenesis and metabolic inefficiency. Biochim Biophys Acta 2001;1504:82–106.
3. Ueno N, Oh-ishi S, Segawa M, *et al.* Effect of age on brown adipose tissue activity in the obese (ob/ob) mouse. Mech Ageing Dev 1998; 100:67–76.
4. Thomas SA, Palmiter RD. Thermoregulatory and metabolic phenotypes of mice lacking noradrenaline and adrenaline. Nature 1996;387: 94–97.
5. Masaki T, Yoshimatsu H, Chiba S, *et al.* Impaired response of UCP family to cold exposure in diabetic (db/db) mice. Am J Physiol Regul Integr Comp Physiol 2000;279:R1305–R1309.
6. Hayashi M, Nagasaka T. Suppression of norepinephrine-induced thermogenesis in brown adipose tissue by fasting. Am J Physiol 1983; 245:E582–E586.
7. Enerback S, Jacobsson A, Simpton EM, *et al.* Mice lacking mitochondrial uncoupling protein are cold-sensitive but not obese. Nature 1996;387:90–94.
8. Cinti S, Frederich RC, Zingaretti MC, *et al.* Immunohistochemical localization of leptin and uncoupling protein in white and brown adipose tissue. Endocrinology 1997;138:797–804.
9. Tein I. Carnitine transport: pathophysiology and metabolism of known molecular defects. J Inherit Metab Dis 2003;26:147–169.

10. Stanley CA, DeLeeuw S, Coates PM, *et al.* Chronic cardiomyopathy and weakness or acute coma in children with a defect in carnitine uptake. Ann Neurol 1991;30:709–716.
11. Nezu J, Tamai I, Oku A, *et al.* Primary systemic carnitine deficiency is caused by mutations in a gene encoding sodium ion-dependent carnitine transporter. Nat Genet 1999;21:91–94.
12. Narama I, Ozaki K, Matsuura T, *et al.* Histopathology of the congenitally carnitine-deficient JVS mouse. Biomed J 1997.
13. Miyagawa J, Kuwajima M, Hanafusa T, *et al.* Mitochondrial abnormalities of muscle tissue in mice with juvenile visceral steatosis associated with systemic carnitine deficiency. Virchows Arch 1995;426:271–279.
14. Kuwajima M, Lu K, Sei M, *et al.* Characteristics of cardiac hypertrophy in the juvenile visceral steatosis mouse with systemic carnitine deficiency. J Mol Cell Cardiol 1998;30:773–781.
15. Kuwajima M, Kono N, Horiuchi M, *et al.* Animal model of systemic carnitine deficiency: analysis in C3H-H-2° strain of mouse associated with juvenile visceral steatosis. Biochem Biophys Res Commun 1991;174:1090–1094.
16. Koizumi T, Nikaido H, Hayakawa J, *et al.* Infantile disease with microvesicular fatty infiltraton of viscera spontaneously occurring in the C3H-H-2° strain of mouse with similarities to Reye's syndrome. Lab Amin 1988;22:83–87.
17. Horiuchi M, Yoshida H, Kobayashi K, *et al.* Cardiac hypertrophy in juvenile visceral steatosis (jvs) mice with systemic carnitine deficiency. FEBS Lett 1993;326:267–271.
18. Horiuchi M, Kobayashi K, Yamaguchi S, *et al.* Primary defect of juvenile visceral steatosis (jvs) mouse with systemic carnitine deficiency is probably in renal carnitine transport system. Biochim Biophys Acta 1994;1226:25–30.
19. Hayakawa J, Koizumi T, Nikaido H. Inheritance of juvenile steatosis of viscera (*jvs*) found in C3H-H-2°. Mouse Genome 1990;86:261.
20. Horiuchi M, Kobayashi K, Tomomura M, *et al.* Carnitine administration to juvenile visceral steatosis mice corrects the suppressed expression of urea cycle enzymes by normalizing their transcription. J Biol Chem 1992;267:5032–5035.
21. Nikaido H, Horiuchi M, Hashimoto N, *et al.* Mapping of jvs (juvenile visceral steatosis) gene, which causes systemic carnitine deficiency in mice, on chromosome 11. Mamm Genome 1995;6:369–370.
22. Takahashi R, Okumura K, Asai T, *et al.* Dietary fish oil attenuates cardiac hypertrophy in lipotoxic cardiomyopathy due to systemic carnitine deficiency. Cardiovasc Res 2005;68:213–223.
23. Wu X, Huang W, Prasad PD, *et al.* Functional characteristics and tissue distribution pattern of organic cation transporter 2 (OCTN2), an organic cation/carnitine transporter. J Pharmacol Exp Ther 1999;290:1482–1492.
24. Tamai I, Ohashi R, Nezu J, *et al.* Molecular and functional identification of sodium ion-dependent, high affinity human carnitine transporter OCTN2. J Biol Chem 1998;273:20378–20382.
25. Lu K, Nishimori H, Nakamura Y, *et al.* A missense mutation of mouse OCTN2, a sodium-dependent carnitine cotransporter, in the juvenile visceral steatosis mouse. Biochem Biophys Res Commun 1998;252:590–594.
26. Yokogawa K, Higashi Y, Tamai I, *et al.* Decreased tissue distribution of L-carnitine in juvenile visceral steatosis mice. J Pharmacol Exp Ther 1999;289:224–230.
27. Yabuuchi H, Tamai I, Nezu J, *et al.* Novel membrane transporter OCTN1 mediates multispecific, bidirectional, and pH-dependent transport of organic cations. J Pharmacol Exp Ther 1999;289:768–773.
28. Wu X, George RL, Huang W, *et al.* Structural and functional characteristics and tissue distribution pattern of rat OCTN1, an organic cation transporter, cloned from placenta. Biochim Biophys Acta 2000;1466:315–327.
29. Nakanishi T, Hatanaka T, Huang W, *et al.* Na^+- and Cl^--coupled active transport of carnitine by the amino acid transporter ATB(0,+) from mouse colon expressed in HRPE cells and Xenopus oocytes. J Physiol 2001;532:297–304.
30. Wang SP, Laurin N, Himms-Hagen J, *et al.* The adipose tissue phenotype of hormone-sensitive lipase deficiency in mice. Obes Res 2001;9:119–128.
31. Slavin BG, Bernick S. Morphological studies on denervated brown adipose tissue. Anat Rec 1974;179:497–506.
32. Osuga J, Ishibashi S, Oka T, *et al.* Targeted disruption of hormone-sensitive lipase results in male sterility and adipocyte hypertrophy, but not in obesity. Proc Natl Acad Sci USA 2000;97:787–792.
33. Holt S, York DA, Fitzsimons JT. The effects of corticosterone, cold exposure and overfeeding with sucrose on brown adipose tissue of obese Zucker rats (fa/fa). Biochem J 1983;214:215–223.
34. Hogan S, Himms-Hagen J. Abnormal brown adipose tissue in obese (ob/ob) mice: response to acclimation to cold. Am J Physiol 1980;239:E301–E309.
35. Sano T, Ozaki K, Matsuura T, *et al.* Giant mitochondria in pancreatic acinar cells of alloxan-induced diabetic rats. Toxicol Pathol 2010;38:658–665.
36. Jalil A, Horiuchi M, Nomoto M, *et al.* Catecholamine metabolism inhibitors and receptor blockades only partially suppress cardiac hypertrophy of juvenile visceral steatosis mice with systemic carnitine deficiency. Life Sci 1999;64:1137–1144.
37. Ellis JM, Li LO, Wu PC, *et al.* Adipose acyl-CoA synthetase-1 directs fatty acids toward beta-oxidation and is required for cold thermogenesis. Cell Metab 2010;12:53–64.
38. Tolwani RJ, Hamm DA, Tian L, *et al.* Medium-chain acyl-CoA dehydrogenase deficiency in gene-targeted mice. PLoS Genet 2005;1:e23.
39. Exil VJ, Gardner CD, Rottman JN, *et al.* Abnormal mitochondrial bioenergetics and heart rate dysfunction in mice lacking very-long-chain acyl-CoA dehydrogenase. Am J Physiol Heart Circ Physiol 2006;290:H1289–H1297.